AIP Applied Physics Letters

The silicon/zinc oxide interface in amorphous silicon-based thin-film solar cells: Understanding an empirically optimized contact

D. Gerlach, R. G. Wilks, D. Wippler, M. Wimmer, M. Lozac'h, R. Félix, A. Mück, M. Meier, S. Ueda, H. Yoshikawa, M. Gorgoi, K. Lips, B. Rech, M. Sumiya, J. Hüpkes, K. Kobayashi, and M. Bär

Citation: Applied Physics Letters **103**, 023903 (2013); doi: 10.1063/1.4813448
View online: http://dx.doi.org/10.1063/1.4813448
View Table of Contents: http://scitation.aip.org/content/aip/journal/apl/103/2?ver=pdfcov
Published by the AIP Publishing

Articles you may be interested in

Micromorph thin-film silicon solar cells with transparent high-mobility hydrogenated indium oxide front electrodes
J. Appl. Phys. **109**, 114501 (2011); 10.1063/1.3592885

Hydrogenated amorphous silicon oxide containing a microcrystalline silicon phase and usage as an intermediate reflector in thin-film silicon solar cells
J. Appl. Phys. **109**, 113109 (2011); 10.1063/1.3592208

Impact of solid-phase crystallization of amorphous silicon on the chemical structure of the buried Si/ZnO thin film solar cell interface
Appl. Phys. Lett. **97**, 072105 (2010); 10.1063/1.3462316

Chemical structure of the (Zn 1 x , Mg x) O / CuIn (S , Se) 2 interface in thin film solar cells
Appl. Phys. Lett. **95**, 122104 (2009); 10.1063/1.3230071

Local versus global absorption in thin-film solar cells with randomly textured surfaces
Appl. Phys. Lett. **93**, 061105 (2008); 10.1063/1.2965117

Re-register for Table of Content Alerts

Create a profile.

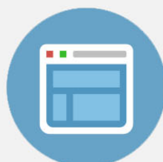
Sign up today!

This article is copyrighted as indicated in the article. Reuse of AIP content is subject to the terms at: http://scitation.aip.org/termsconditions. Downloaded to IP: 160.45.66.177 On: Wed, 02 Apr 2014 07:19:33

The silicon/zinc oxide interface in amorphous silicon-based thin-film solar cells: Understanding an empirically optimized contact

D. Gerlach,[1] R. G. Wilks,[1] D. Wippler,[2] M. Wimmer,[1] M. Lozac'h,[3] R. Félix,[1] A. Mück,[2] M. Meier,[2] S. Ueda,[3] H. Yoshikawa,[4] M. Gorgoi,[1] K. Lips,[1] B. Rech,[1] M. Sumiya,[3] J. Hüpkes,[2] K. Kobayashi,[5] and M. Bär[1,6]

[1]*Helmholtz-Zentrum Berlin für Materialien und Energie GmbH, Hahn-Meitner-Platz 1, D-14109 Berlin, Germany*
[2]*Institut für Energie- und Klimaforschung, Forschungszentrum Jülich GmbH, Wilhelm-Johnen-Straße, D-52428 Jülich, Germany*
[3]*National Institute for Materials Science (NIMS), 1-1 Namiki, Tsukuba, Ibaraki 305-0044, Japan*
[4]*Synchrotron X-ray Station at SPring-8, NIMS, Kouto 1-1-1, Sayo-cho, Sayo-gun, Hyogo 679-5148, Japan*
[5]*Quantum Beam Science Directorate, Japan Atomic Energy Agency, Kouto 1-1-1, SPring-8, Sayo-cho, Sayo-gun, Hyogo 679-5148, Japan*
[6]*Institut für Physik und Chemie, Brandenburgische Technische Universität Cottbus, Konrad-Wachsmann-Allee 1, D-03046 Cottbus, Germany*

(Received 7 May 2013; accepted 16 June 2013; published online 9 July 2013)

The electronic structure of the interface between the boron-doped oxygenated amorphous silicon "window layer" (a-SiO_x:H(B)) and aluminum-doped zinc oxide (ZnO:Al) was investigated using hard x-ray photoelectron spectroscopy and compared to that of the boron-doped microcrystalline silicon (μc-Si:H(B))/ZnO:Al interface. The corresponding valence band offsets have been determined to be (-2.87 ± 0.27) eV and (-3.37 ± 0.27) eV, respectively. A lower tunnel junction barrier height at the μc-Si:H(B)/ZnO:Al interface compared to that at the a-SiO_x:H(B)/ZnO:Al interface is found and linked to the higher device performances in cells where a μc-Si:H(B) buffer between the a-Si:H p-i-n absorber stack and the ZnO:Al contact is employed. © *2013 AIP Publishing LLC.*
[http://dx.doi.org/10.1063/1.4813448]

In the advancing field of thin-film photovoltaics (PV), the cost-efficient production methods associated with hydrogenated amorphous silicon (a-Si:H) technology ensures that it will remain a major part of a consolidating PV market.[1] The highest efficiencies in amorphous silicon p-i-n solar cells are currently achieved with ZnO-based transparent conductive oxide (TCO) as a front contact.[2] Previous (mainly empirical) work has shown that the cell efficiency can be increased significantly[3,4] by introducing a p-type microcrystalline Si (μc-Si:H) buffer between the a-Si:H p-i-n layer stack and aluminum-doped ZnO (ZnO:Al) TCO (see Fig. 1). This suggests an unfavorable electronic p-type a-Si:H/ZnO:Al interface structure as a limiting factor in related solar cell devices. State-of-the-art a-Si:H p-i-n solar cells additionally employ a p-type *oxygenated* a-Si:H (a-SiO_x:H(B)) emitter to enhance transmission through this "window layer"[5] (also depicted in Fig. 1).

In order to examine the Si/ZnO contact properties and explain the observed influence of the μc-Si:H buffer layer on cell performance, hard x-ray photoelectron spectroscopy (HAXPES) was utilized to probe the electronic structure of the buried interface between ZnO:Al TCO and boron-doped a-SiO_x:H or μc-Si:H layers. By varying the x-ray excitation energy and Si thicknesses, different portions of the layer stack can be probed,[6] allowing the buried interface to be studied while minimizing the influence of surface contaminants/oxidation on the measurements, as we discussed in some detail in previous work.[6] It was shown using surface-sensitive Si 1s spectra that a pronounced downward band bending is presumably limited to the very surface region of the investigated a-SiO_x:H(B)/ZnO:Al and μc-Si:H(B)/ZnO:Al layer stacks. To avoid this unwanted influence of the *surface* on the determination of the electronic *interface* structure, the current study focuses on more bulk-sensitive photoemission lines.

ZnO:Al layers were rf sputter-deposited onto Corning Eagle® XG glass from a planar ceramic ZnO:Al_2O_3 (99:1 wt/wt%) target in an in-line sputtering system using a substrate temperature of 300 °C and 0.1 Pa pure argon.[8] Using plasma-enhanced chemical vapor deposition (PECVD), thin, boron-doped, hydrogenated, and oxygenated amorphous [a-SiO_x:H(B)] and microcrystalline [μc-Si:H(B)] layers were deposited onto the ZnO:Al TCO using standard conditions for the preparation of p-type Si layers in superstrate solar cells.[9] Mixtures of SiH_4, $B(CH_3)_3$, H_2 (and CO_2) precursor gases were used at flow rates of 20.8/0.35/120(/42) sccm

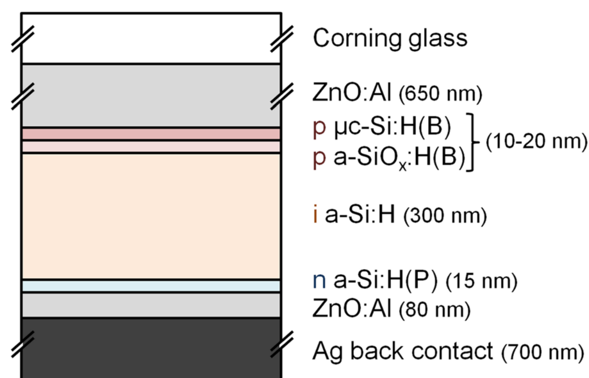

FIG. 1. Schematic of a glass/ZnO:Al/p-i-n a-Si:H/ZnO:Al/Ag thin-film solar cell with a μc-Si:H(B) buffer layer and a p-type a-SiO_x:H window (modified from Ref. 7).

 © 2013 AIP Publishing LLC

This article is copyrighted as indicated in the article. Reuse of AIP content is subject to the terms at: http://scitation.aip.org/termsconditions. Downloaded to IP: 160.45.66.177 On: Wed, 02 Apr 2014 07:19:33

(standard cubic centimeters per minute) and 2.7/0.012/1010 sccm for the deposition of a-SiO_x:H(B) and μc-Si:H(B) layers, respectively. By varying the PECVD process time, "thin" layers with thicknesses of 12.8 nm [a-SiO_x:H(B)] or 13.2 nm [μc-Si:H(B)] were grown, as well as "thick" samples with 30.4 nm [a-SiO_x:H(B)] or 38.5 nm [μc-Si:H(B)] layers. The thicknesses were determined based on the attenuation of Zn-related photoemission lines and verified by spectral ellipsometry measurements.[6] HAXPES measurements were performed at the bending magnet Beamline KMC-1 (Ref. 10) (equipped with a double-crystal monochromator) of the BESSY II synchrotron light source using the HIKE endstation[11] and at BL15XU[12] of SPring-8 (equipped with a helical undulator and a double-crystal monochromator). At both beamlines a VG SCIENTA R4000 hemispherical analyzer is used for electron detection. BL15XU delivers higher x-ray intensities and HAXPES energy resolution.[13] Initial investigations were performed on some selected samples at SPring-8; however, as the complete sample set was characterized at KMC-1, following discussions and spectra are based on data acquired at BESSY II (if not stated otherwise).

Energy scales were calibrated using Au 4f core level and Au Fermi edge (E_F) measurements. Stated energy-scale error bars were estimated based on the beamline resolution,[10] the standard deviation of respective curve fits and data quality (i.e., signal-to-noise ratio). Valence band (VB) and core level spectra were measured for every sample at various excitation energies.

Figure 2 shows the VB spectra of the thick (30.4 nm) a-SiO_x:H(B) layer, the thick (38.5 nm) μc-Si:H(B) layer (both on ZnO:Al) and the bare ZnO:Al TCO. For the TCO both the spectra acquired at BESSY II (△) and SPring-8 (-▽-) are shown. The spectra measured at BESSY II were normalized to the maximum intensity in the -9 to 0 eV range. The TCO spectrum taken at SPring-8 was scaled such that the integral intensities in that region are equal for the spectra taken at BESSY II and SPring-8. For both thin-film Si samples the region between -5 and -1 eV can be ascribed to the valence states of the Si capping layer.[14] The valence band maximum (VBM) of the thick μc-Si:H(B) layer is at lower binding energy, i.e., closer to E_F than that of a-SiO_x:H(B). Estimating the VBM value[15] from the intersection of the linear approximation of the leading edge of the VB spectrum and the background results in VBM values of (-0.77 ± 0.10) eV for a-SiO_x:H(B) and (-0.25 ± 0.10) eV for μc-Si:H(B). Note that in Ref. 6, we reported a pronounced downward band bending presumably limited to the very surface of the same SiO_x:H(B) and μc-Si:H(B) layers studied here. This effect was found to be more pronounced for μc-Si:H(B). Despite the significantly higher bulk sensitivity of the VB measurements (compared to the high-binding energy Si 1s core levels studied in Ref. 6), a potential impact of the observed downward surface band bending[6] on the VBM must be considered. The significant "tail" region which can be observed for the μc-Si:H(B) samples might thus be explained by this more pronounced surface band bending. Downward surface band bending means that the VBM moves away from E_F nearer the surface, and therefore we take the very leading edge of the measured VBM region as being representative of the "real" VBM.

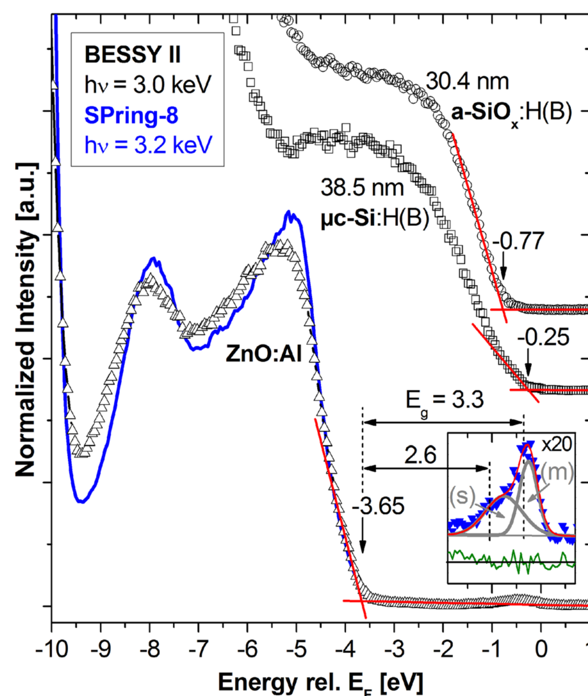

FIG. 2. HAXPES spectra (recorded with excitation energies of 3.0 and 3.2 keV) of the valence band region of the 30.4 nm thick a-SiO_x:H(B) (top spectrum, ○), the 38.5 nm thick μc-Si:H(B) layer (center spectrum, □), and the bare ZnO:Al TCO (bottom spectra). Note that for the last both the BESSY II (△) and SPring-8 (-▼-) data are presented. The VBMs are determined by linear approximation of the leading edge (red lines); the experimental uncertainty of the derived VBM values is ±0.10 eV for the Si and ±0.15 eV for the ZnO:Al data. The inset magnifies the spectral region around the Fermi edge, E_F, of the SPring-8 ZnO:Al TCO data on the same energy scale. A two-component fit (red curve) together with the residuum is also shown. The optical band gap (Refs. 16 and 17) $E_g = 3.3$ eV, of undoped ZnO and 2.6 eV (representing the prominent "blue-green" luminescence reported in literature (Refs. 18–20) are indicated relative to VBM. Note that the respective arrows do not represent the actual distance to the main (m) and secondary (s) above-VBM feature.

The VB spectra of the bare ZnO:Al TCO exhibit (for both the BESSY II and SPring-8 data) an onset at (-3.65 ± 0.15) eV. The optical band gap for *undoped* ZnO is reported to be $E_g = 3.3$ eV (Refs. 16 and 17) which is significantly lower than the derived VBM. However, highly doped ZnO:Al exhibits a Burstein-Moss shift of E_F into the conduction band (CB),[21,22] resulting in optical band gap values of up to 3.8 eV.[23] We detect significant spectral intensity above the VBM near E_F. The inset of Fig. 2 shows a magnification of the respective range of the higher-resolution spectrum[13] taken at SPring-8. In a first approximation[24] the asymmetry of this contribution was accounted for by a fit using two Voigt profiles and a linear background. The shape of the peak is well-represented in this way; the fit is optimized when the main peak (m) is centered at (-0.26 ± 0.10) eV and the secondary peak (s) is at (-0.8 ± 0.2) eV. The separation between the main peak and the previously determined VBM [$\Delta E = (3.39 \pm 0.14)$ eV] corresponds (within the error bar) to the reported optical band gap of undoped ZnO ($E_g = 3.3$ eV,[16,17] as indicated in the inset of Fig. 2).

The ratio of the intensity of the main peak (I_m) of the above-VBM feature to that of the O 2p VB states (I_{VB}, in the range of -9 eV to -4 eV) I_m/I_{VB} is (2.1 ± 0.5)‰. Note that as in Refs. 25 and 26, we assume similar photoionization cross

This article is copyrighted as indicated in the article. Reuse of AIP content is subject to the terms at: http://scitation.aip.org/termsconditions. Downloaded to IP: 160.45.66.177 On: Wed, 02 Apr 2014 07:19:33

sections for the above-VBM and O 2p VB. The VB electron density of ZnO can be calculated by $n_{VB} = 6 \times \rho \times N_a/M$ [with the density of ZnO $\rho = 5.68\,\mathrm{g\,cm^{-3}}$,[27] the Avogadro constant $N_a = 6.02 \times 10^{23}\,\mathrm{mol^{-1}}$, the number of valence electrons (6) and the molar mass of ZnO $M = 81.39\,\mathrm{g\,mol^{-1}}$][27] to be $2.52 \times 10^{23}\,\mathrm{cm^{-3}}$. Hall measurements of our ZnO:Al thin films typically indicate carrier concentrations of $n_e = (5 \pm 1) \times 10^{20}\,\mathrm{cm^{-3}}$ (Ref. 28), and thus the corresponding n_e/n_{VB} ratio is (2.0 ± 0.5)‰. Comparing n_e/n_{VB} with the computed I_m/I_{VB} intensity ratio reveals an excellent agreement (note that I_{m+s}/I_{VB} is significantly larger),[29] suggesting that the main peak contribution (m) of the above-VBM feature exclusively represents occupied conduction band states.[24]

Occupied states within the band gap of degenerated ZnO:Al films and for undoped ZnO were previously observed using HAXPES by Li *et al.*;[25] the intensity of the above-VBM features in the HAXPES measurements for the undoped ZnO were significantly lower, and all were attributed to oxygen vacancies (V_O). For ZnO (Refs. 18 and 19) and ZnO:Al (Ref. 20) a prominent 2.6 eV (blue-green) luminescence is reported in literature. The origin of this luminescence is still under debate—V_O states and/or zinc vacancies are the most likely candidates.[30] The 2.6 eV luminescence coincides (within the experimental uncertainty) with a transition between the VBM and the secondary peak of our above-VBM feature: $3.65\,\mathrm{eV} - 0.8\,\mathrm{eV} = (2.85 \pm 0.22)\,\mathrm{eV}$ (see inset of Fig. 2). Considering this, the observed secondary feature (s) may be attributable to localized (trapped) electrons in defect states within the gap. Thus, we would interpret the above-VBM feature as a superposition of occupied conduction band [→ feature (m)] and defect-related [→ feature (s)] states. This explanation can be reconciled with the conclusions of Li *et al.*[25] if the doping/charge carrier concentrations of the studied ZnO:Al material differ significantly (i.e., higher in the current case).

In a first approximation, the separations between the VBM of the TCO and the Si cover layers provide estimates of the valence band offsets (VBO) at the respective interfaces [neglecting any impact of an interface induced band bending (IIBB)]. For the a-SiO_x:H(B)/ZnO:Al and the μc-Si:H(B)/ZnO:Al interfaces, we thus estimate VBO values of (-2.88 ± 0.18) eV and (-3.40 ± 0.18) eV, respectively.

To account for any IIBB, we used the procedure described in Ref. 31. The Si 2s and Zn 3s core level spectra of the thin (bottom panels) and thick (top panels) Si samples and the bare ZnO:Al (center panels) were measured and are shown in Fig. 3. For the thick Si samples only a Si 2s contribution can be observed, while for the ZnO:Al only a Zn 3s contribution is detectable. The thin Si samples show a dominant Si 2s line, but close inspection reveals an additional contribution from Zn 3s photoemission from the buried ZnO:Al substrate. The Si 2s line exhibits a shoulder at higher binding energies that is more pronounced for thin samples and a-SiO_x:H(B). For a more detailed evaluation, all spectra were fitted simultaneously with two Voigt profiles for Si 2s and one single Voigt profile for Zn 3s including a linear

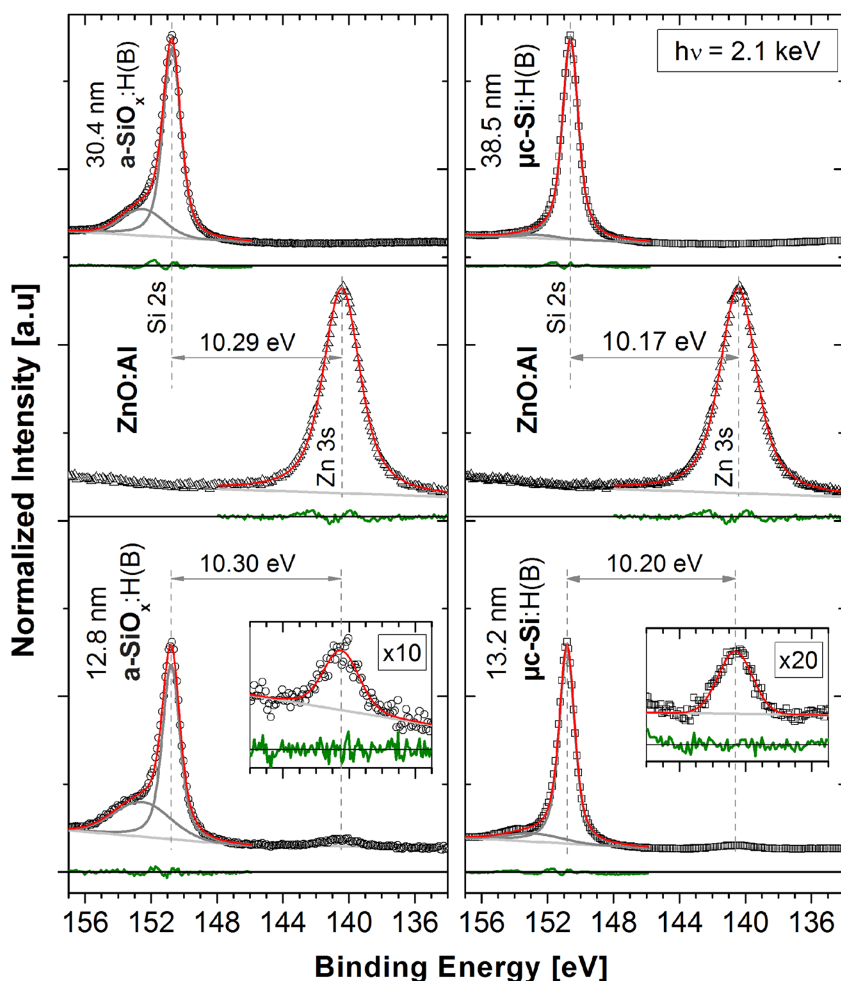

FIG. 3. Si 2s and Zn 3s HAXPES spectra of a-SiO_x:H(B) (left panels) and μc-Si:H(B) (right panels) measured at 2.1 keV excitation energy. The spectra of the thinnest (bottom panel) and thickest (top panel) Si layers are compared to that of the bare ZnO:Al substrate (identical spectra; center panels). The Si 2s and Zn 3s peaks were fitted with Voigt profiles including a linear background. Dots represent the measured data and lines the fit (red), individual contributions (gray), and residua (green). The insets show a magnification of the Zn 3s region for the thin samples. Fitted line positions are indicated and values for the Si 2s–Zn 3s energy difference are given (±0.14 eV).

This article is copyrighted as indicated in the article. Reuse of AIP content is subject to the terms at: http://scitation.aip.org/termsconditions. Downloaded to IP: 160.45.66.177 On: Wed, 02 Apr 2014 07:19:33

background. Comparing the binding energies with reference data,[32] the high and low binding energy Si 2s components can be ascribed to Si-O_x and Si-Si bonds, respectively, and the Zn 3s photoemission line can be attributed to ZnO. In the case of μc-Si:H(B), the presence of Si-O_x bonds can mainly be attributed to surface oxidization. For the a-SiO_x:H(B) layer a significantly higher Si-O_x contribution is present due to the deliberate material oxygenation. From the fit of the thick a-SiO_x:H(B) samples a Si-O_x/Si-Si intensity fraction of (26 ± 2)% can be derived. However, this fraction must be considered a higher-bound approximation of the "true" Si-O_x bulk contribution because of the impact of surface oxides on the intensity ratio. Note that both thin Si samples exhibit a higher Si-O_x contribution, presumably due to the higher surface/bulk ratio and, potentially, the previously observed oxidation at the Si/ZnO:Al interface.[6,33,34]

The IIBB is determined by subtracting the binding energy difference between the core levels of the capping layer and the substrate of the thin silicon sample [e.g., $E_{Si\,2s}$ (12.8 nm a-SiO_x:H(B)) – $E_{Zn\,3s}$ (12.8 nm a-SiO_x:H(B)) = (10.30 $\pm$ 0.14) eV] from the respective energy difference of the cover layer core level of a thick silicon layer and the substrate core level of the bare substrate reference [e.g., $E_{Si\,2s}$ (30.4 nm a-SiO_x:H(B)) – $E_{Zn\,3s}$ (ZnO:Al) = (10.29 ± 0.14) eV]. We calculate an IIBB of (0.01 ± 0.20) eV for the a-SiO_x:H(B)/ZnO:Al and (0.03 ± 0.20) eV for the μc-Si:H(B)/ZnO:Al layer stack.

Subtracting the IIBB from the difference of the VBM values of Si and ZnO:Al finally results in the VBO of (-2.87 ± 0.27) eV for the a-SiO_x:H(B)/ZnO:Al and (-3.37 ± 0.27) eV for the μc-Si:H(B)/ZnO:Al interface. A schematic presentation of the resulting electronic structure of the Si/ZnO:Al interfaces is shown in Fig. 4. As the electrical contact at this interface is achieved through a tunnel junction,[35] not the derived VBO values but rather the energetic distance between Si VBM and ZnO:Al CB minimum, CBM (i.e., the tunnel junction barrier height, eV_b), determines the electronic quality of this contact. To approximate the ZnO:Al CBM position, the optical band gap of the undoped ZnO

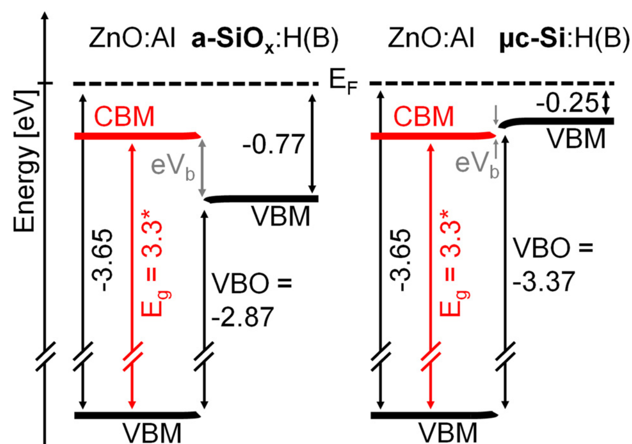

FIG. 4. Schematic of the electronic structure of the a-SiO_x:H(B)/ZnO:Al and μc-Si:H(B)/ZnO:Al interfaces based on HAXPES measurements. The stated values are all in eV and the experimental uncertainty of the derived VBM values is $\pm$0.10 eV for the Si data, $\pm$0.15 eV for the ZnO:Al data, and $\pm$0.27 eV for the VBOs. The indicated IIBB is not to scale (* to estimate the relative position of the ZnO:Al CBM, the band gap value of *undoped* ZnO (Refs. 16 and 17) is included).

($E_g = 3.3$ eV)[16,17] was used and added to the corresponding VBM value. eV_b can then be estimated by adding the (negative) VBO to E_g. We find a lower barrier height for the μc-Si:H(B)/ZnO:Al interface [(-0.07 ± 0.27) eV] than for the a-SiO_x:H(B)/ZnO:Al interface [(0.43 ± 0.27) eV]. Moreover, the lower doping efficiency found in amorphous silicon[36] compared to that in microcrystalline silicon could result in a much larger depletion width of the space charge region at the interface and therefore a larger tunnel distance for holes. Thus, charge transport across the Si/ZnO tunnel junction is energetically more favorable for the μc-Si:H(B)/ZnO:Al than for the a-SiO_x:H(B)/ZnO:Al interface.

The practical effect of such a difference in a solar cell device is that the photogenerated holes are more likely to tunnel into the TCO front contact (where they can contribute to the current) if a p-type μc-Si:H(B) is used as a buffer between the a-Si:H p-i-n cell and the ZnO:Al TCO. This finding might explain the underlying mechanism for the empirically found better performance of a-Si:H p-i-n based solar cells employing a μc-Si:H(B) buffer.

In summary, HAXPES valence band spectra revealed that the investigated ZnO:Al layer is degenerated, with the Fermi level lying within the conduction band. The valence band offsets at the a-SiO_x:H(B)/ZnO:Al and the μc-Si:H(B)/ZnO:Al interfaces were found to be (-2.87 ± 0.27) eV and (-3.37 ± 0.27) eV, respectively. Using the measured position of the valence band maximum of ZnO:Al and the reported optical band gap energy of *undoped* ZnO, the position of the conduction band minimum of the ZnO:Al TCO was approximated. Together with the measured valence band offsets, the tunnel junction barrier height between the valence band maximum of the silicon layers and the conduction band minimum of the ZnO:Al TCO was estimated. The lower barrier height for the μc-Si:H(B)/ZnO:Al interface corresponds to the previously reported[3,4] increase in solar cell efficiency when a μc-Si:H(B) buffer is introduced between a-Si:H p-i-n absorber stack and ZnO:Al front contact. Based on the methods and findings described here, it is expected that further knowledge-based optimization of the p-type a-Si:H/ZnO:Al interface will result in higher efficiencies of amorphous Si thin-film PV devices.

This work was supported in part by the Helmholtz-Association (VH-NG-423) and the German Federal Ministry of the Environment (BMU, Contract Nos. 0327693 and 0325299). The HAXPES measurements at SPring-8 were performed under the approval of NIMS Beamline Station (Proposal Nos. 2011A4609 and 2012B4610). S.U. would like to thank HiSOR, Hiroshima University and JAEA/SPring-8 for the development of HAXPES at BL15XU of SPring-8.

[1] A. Shah, J. Meier, A. Buechel, U. Kroll, J. Steinhauser, F. Meillaud, H. Schade, and D. Dominé, Thin Solid Films **502**, 292 (2006).
[2] S. Benagli, D. Borrello, E. Vallat-Sauvain, J. Meier, U. Kroll, J. Hötzel, J. Bailat, J. Steinhauser, M. Marmelo, G. Monteduro, and L. Castens, in *EUPVSEC Proceedings*, 2009, pp. 2293–2298.
[3] J. Müller, O. Kluth, S. Wieder, H. Siekmann, G. Schöpe, W. Reetz, O. Vetterl, D. Lundszien, A. Lambertz, F. Finger, B. Rech, and H. Wagner, Sol. Energy Mater. Sol. Cells **66**, 275 (2001).
[4] J. C. Lee, V. Dutta, J. Yoo, J. Yi, J. Song, and K. H. Yoon, Superlattice Microstruct. **42**, 369 (2007).

This article is copyrighted as indicated in the article. Reuse of AIP content is subject to the terms at: http://scitation.aip.org/termsconditions. Downloaded to IP: 160.45.66.177 On: Wed, 02 Apr 2014 07:19:33

[5]R. Biron, C. Pahud, F.-J. Haug, J. Escarré, K. Söderström, and C. Ballif, J. Appl. Phys. **110**, 124511 (2011).
[6]D. Gerlach, D. Wippler, R. G. Wilks, M. Wimmer, M. Lozac'h, R. Félix, S. Ueda, H. Yoshikawa, K. Lips, B. Rech, M. Sumiya, K. Kobayashi, M. Gorgoi, J. Hüpkes, and M. Baür, IEEE J. Photovoltaics **3**, 483 (2013).
[7]M. Kubon, E. Boehmer, F. Siebke, B. Rech, C. Beneking, and H. Wagner, Sol. Energy Mater. Sol. Cells **41–42**, 485 (1996).
[8]M. Berginski, J. Hüpkes, M. Schulte, G. Schöpe, H. Stiebig, B. Rech, and M. Wuttig, J. Appl. Phys. **101**, 074903 (2007).
[9]B. Rech and H. Wagner, Appl. Phys. A **69**, 155 (1999).
[10]F. Schaefers, M. Mertin, and M. Gorgoi, Rev. Sci. Instrum. **78**, 123102 (2007).
[11]M. Gorgoi, S. Svensson, F. Schäfers, G. Öhrwall, M. Mertin, P. Bressler, O. Karis, H. Siegbahn, A. Sandell, H. Rensmo, W. Doherty, C. Jung, W. Braun, and W. Eberhardt, Nucl. Instrum. Methods A **601**, 48 (2009).
[12]S. Ueda, Y. Katsuya, M. Tanaka, H. Yoshikawa, Y. Yamashita, S. Ishimaru, Y. Matsushita, and K. Kobayashi, AIP Conf. Proc. **1234**, 403 (2010).
[13]The experimental resolution (as determined by a fit of the Fermi edge of a clean gold foil) of the 3 keV BESSY II and the 3.2 keV SPring-8 data is 480 and 210 meV, respectively.
[14]R. A. Street, *Hydrogenated Amorphous Silicon* (Cambridge University Press, 2005).
[15]D. Eich, K. Ortner, U. Groh, Z. H. Chen, C. R. Becker, G. Landwehr, R. Fink, and E. Umbach, Phys. Status Solidi A **173**, 261 (1999).
[16]K. H. Kim, K. C. Park, and D. Y. Ma, J. Appl. Phys. **81**, 7764 (1997).
[17]M. Suchea, S. Christoulakis, N. Katsarakis, T. Kitsopoulos, and G. Kiriakidis, Thin Solid Films **515**, 6562 (2007).
[18]K. Vanheusden, W. L. Warren, C. H. Seager, D. R. Tallant, J. A. Voigt, and B. E. Gnade, J. Appl. Phys. **79**, 7983 (1996).
[19]J. H. Noh, I.-S. Cho, S. Lee, C. M. Cho, H. S. Han, J.-S. An, C. H. Kwak, J. Y. Kim, H. S. Jung, J.-K. Lee, and K. S. Hong, Phys. Status Solidi A **206**, 2133 (2009).
[20]E. M. Likovich, R. Jaramillo, K. J. Russell, S. Ramanathan, and V. Narayanamurti, Appl. Phys. Lett. **99**, 151910 (2011).
[21]E. Burstein, Phys. Rev. **93**, 632 (1954).
[22]T. S. Moss, Proc. Phys. Soc., Sec. B **67**, 775 (1954).
[23]W. Yang, Z. Wu, Z. Liu, A. Pang, Y.-L. Tu, and Z. C. Feng, Thin Solid Films **519**, 31 (2010).
[24]If the main peak of the above-VBM feature is due to occupied conduction band states, then it should be described by a convolution of a square-root (representing the parabolic conduction band density) and Fermi function (as suggested in Ref. 26). Thus the fitting procedure used here, with two Voigt profiles and a linear background, is a rather coarse approach but has no significant effect on the determined band alignment.
[25]B. Li, Y. Adachi, J. Li, H. Okushi, I. Sakaguchi, S. Ueda, H. Yoshikawa, Y. Yamashita, S. Senju, K. Kobayashi, M. Sumiya, H. Haneda, and N. Ohashi, Appl. Phys. Lett. **98**, 082101 (2011).
[26]K. Nomura, T. Kamiya, H. Yanagi, E. Ikenaga, K. Yang, K. Kobayashi, M. Hirano, and H. Hosono, Appl. Phys. Lett. **92**, 202117 (2008).
[27]S. Adachi, *Handbook on Physical Properties of Semiconductors* (Springer, 2004).
[28]M. Berginski, J. Hüpkes, W. Reetz, B. Rech, and M. Wuttig, Thin Solid Films **516**, 5836 (2008).
[29]The ratio of the total integral intensity (I_{m+s}) of the above-VBM feature to I_{VB} is (4.4 ± 0.5)‰.
[30]A. Janotti and C. G. V. de Walle, Rep. Prog. Phys. **72**, 126501 (2009).
[31]M. Bär, B.-A. Schubert, B. Marsen, R. G. Wilks, S. Pookpanratana, M. Blum, S. Krause, T. Unold, W. Yang, L. Weinhardt, C. Heske, and H.-W. Schock, Appl. Phys. Lett. **99**, 222105 (2011).
[32]See http://srdata.nist.gov/xps/Default.aspx for "National Institute of Standards and Technology X-ray Photoelectron Spectroscopy Database."
[33]M. Wimmer, M. Bär, D. Gerlach, R. G. Wilks, S. Scherf, C. Lupulescu, F. Ruske, R. Félix, J. Hüpkes, G. Gavrila, M. Gorgoi, K. Lips, W. Eberhardt, and B. Rech, Appl. Phys. Lett. **99**, 152104 (2011).
[34]M. Bär, M. Wimmer, R. G. Wilks, M. Roczen, D. Gerlach, F. Ruske, K. Lips, B. Rech, L. Weinhardt, M. Blum, S. Pookpanratana, S. Krause, Y. Zhang, C. Heske, W. Yang, and J. D. Denlinger, Appl. Phys. Lett. **97**, 072105 (2010).
[35]K. Ellmer, A. Klein, and B. Rech, *Transparent Conductive Zinc Oxide: Basics and Applications in Thin Film Solar Cells* (Springer, 2008), p. 24.
[36]K. Winer, R. A. Street, N. M. Johnson, and J. Walker, Phys. Rev. B **42**, 3120 (1990).

This article is copyrighted as indicated in the article. Reuse of AIP content is subject to the terms at: http://scitation.aip.org/termsconditions. Downloaded to IP: 160.45.66.177 On: Wed, 02 Apr 2014 07:19:33